doubtedly reflects a fundamental internal energy difference related to the anomeric stereochemistry. We have sought to use the calculated transition-state energies to demonstrate this.

The analysis in Figures 1 and 2 can be conveniently summarized as shown in Scheme VI, and this display suggests a method for testing the validity of the entire investigation. We have determined the energy difference between the transition-state strctures **10** and **11** to be 1.05 kcal (6-31G*//6-31G*, Scheme VI). The difference in ground-state energies for glycosides **8** and **9** has been found by us to be 1.47 kcal (6-31G*//6-31G*).[27] On the assumption that entropies and solvation energies are the same for the α and β anomers, the Arrhenius equation can be applied as shown in Scheme VI to compare relative rate constants for axial and equatorial cleavage—assuming that the preexponential factors are equal. For a temperature of 75 °C, the above treatment predicts that β/α rate ratio should be 1.8 and is therefore in good agreement with the data in Table I. For a temperature of 23 °C, the predicted ratio is 1.9, and this agrees with the value of 2.0 obtained for the restrained anomers studied by us.[10]

The good agreement between calculated and observed rate constants suggests that our transition-state analyses are credible and, by corollary, that the transition-state structures in hydrolysis of axial and equatorial glycosides are $^4H_3$ and ^4E, respectively. Our results offer more refined conformational analysis than that obtained in the elegant kinetics studies of Bennet and Sinnott.[27] That $n\sigma^*$ interactions play a profound role in oxygen basicities[11] and bond reorganizations is apparent from our studies. A full investigation of these effects and their roles in competing reaction pathways, e.g., endo vs exo glycoside cleavage, is underway and will be reported in due course.

Acknowledgment. This work was supported by grants from the National Science Foundation (CHE 8703916) and National Institutes of Health (GM-41071) to B.F.-R. and from the North Carolina Supercomputing Center to B.F.-R., J.P.B., and C.W.A. We thank the Biological Instrumentation Program (NSF) for use of the Convex C220 at the University of North Carolina, Chapel Hill.

Registry No. 3, 72036-48-7; **8** (H^+), 135789-43-4; **9** (H^+), 135789-44-5.

(29) See for example: Hough, L.; Richardson, A. C. In *Comprehensive Organic Chemistry*; Ed. Barton, D., Ollis, W. D., Eds.; Pergamon: Oxford, 1974; Vol. V, p 692. For the alternative usage, see *Principles of Organic Stereochemistry*; Testa, B. Ed.; Dekker: New York, 1979; p 86.

Optical Activity Arising from ^{13}C Substitution: Vibrational Circular Dichroism Study of (2*S*,3*S*)-Cyclopropane-*1*-^{13}C,^2H-*2*,*3*-$^2H_2$

Teresa B. Freedman,* Steven J. Cianciosi, N. Ragunathan, John E. Baldwin, and Laurence A. Nafie

Contribution from the Department of Chemistry, Syracuse University, Syracuse, New York 13244-4100. *Received January 18, 1991*

Abstract: Vibrational circular dichroism (VCD) spectra of the novel chiral compound (2*S*,3*S*)-cyclopropane-*1*-^{13}C,^2H-*2*,*3*-$^2H_2$ (**1**) are reported. This quadruply labeled cyclopropane is chiral due to substitution of ^{13}C at carbon 1 of *anti*-cyclopropane-*1*,*2*,*3*-$^2H_3$ (**2**). In C_2Cl_4 solution, a conservative (+,−,+) VCD pattern is observed in both the CH and CD stretching regions. From normal-coordinate analysis, these VCD bands are found to arise from chiral perturbation which mixes the A′ and A″ symmetry modes of **2**. Excellent quantitative agreement with the experimental VCD spectra is obtained by applying a generalized coupled-oscillator model to the motions of the two pairs of chirally oriented trans CH or CD oscillators.

Introduction

Chirality can be introduced into a nondissymmetric molecule by nuclear isotopic substitution that makes it dissymmetric by eliminating reflection, inversion, or, more generally, S_n symmetry. Several molecules that are chiral due to deuterium substitution have been investigated[1-8] by vibrational circular dichroism (VCD) spectroscopy.[9-13] In these cases, the heavier mass of the deuterium causes an ~800-cm^{-1} decrease in the CH stretching frequency and significant shifts in the CH bending frequencies as well, resulting in modes in which the CH and CD motions are largely uncoupled from each other. The VCD bands, in most cases, can be attributed to the coupled motion of chirally oriented CH or CD oscillators.[2-6]

Substitution of ^{13}C for ^{12}C results in an ~9-cm^{-1} decrease in the CH stretching frequency, an ~7-cm^{-1} decrease in the fre-

(1) Polavarapu, P. L.; Nafie, L. A.; Benner, S. A.; Morton, T. H. *J. Am. Chem. Soc.* **1981**, *103*, 5349.
(2) Annamalai, A.; Keiderling, T. A.; Chickos, J. S. *J. Am. Chem. Soc.* **1984**, *106*, 6254.
(3) Annamalai, A.; Keiderling, T. A.; Chickos, J. S. *J. Am. Chem. Soc.* **1985**, *107*, 2285.
(4) Freedman, T. B.; Paterlini, M. G.; Lee, N.-S.; Nafie, L. A.; Schwab, J. M.; Ray, T. *J. Am. Chem. Soc.* **1987**, *109*, 4727.
(5) Cianciosi, S. J.; Spencer, K. M.; Freedman, T. B.; Nafie, L. A.; Baldwin, J. E. *J. Am. Chem. Soc.* **1989**, *111*, 1913.
(6) Freedman, T. B.; Spencer, K. M.; McCarthy, C.; Cianciosi, S. J.; Baldwin, J. E.; Nafie, L. A.; Moore, J. A.; Schwab, J. M. *Proc. SPIE-Int. Soc. Opt. Eng.* **1989**, *1145*, 273.
(7) Spencer, K. M.; Cianciosi, S. J.; Baldwin, J. E.; Freedman, T. B.; Nafie, L. A. *Appl. Spectrosc.* **1990**, *44*, 235.
(8) Cianciosi, S. J.; Ragunathan, N.; Freedman, T. B.; Nafie, L. A.; Baldwin, J. E. *J. Am. Chem. Soc.* **1990**, *112*, 8204.
(9) Freedman, T. B.; Nafie, L. A. In *Topics in Stereochemistry*; Eliel, E., Wilen, S., Eds.; Wiley: New York, 1987; Vol. 17, pp 113-206.
(10) Stephens, P. J.; Lowe, M. A. *Annu. Rev. Phys. Chem.* **1985**, *36*, 213.
(11) Keiderling, T. A. In *Practical Fourier Transform Infrared Spectroscopy*; Ferraro, J. R., Krishnan, K., Eds.; Academic Press: San Diego, CA, 1990; pp 203-283.
(12) Polavarapu, P. L. In *Vibrational Spectra and Structure*; Durig, J. R., Ed.; Elsevier: Amsterdam, 1984; Vol. 13, pp 103-160.
(13) Nafie, L. A. In *Advances in Infrared and Raman Spectroscopy*; Clark, R. J. M., Hester, R. E., Eds.; Wiley-Heyden: London, 1984; Vol. 11, p 49.

0002-7863/91/1513-8298$02.50/0

Table I. Observed and Calculated Absorption and VCD Spectra of (2*S*,3*S*)-Cyclopropane-*1*-^{13}C,^{2}H-*2*,*3*-$^{2}H_2$

obsd[a]				calcd[b-d]		
freq, cm^{-1}	ϵ, 10^3 cm^2 mol^{-1}	$10^3\Delta\epsilon$, 10^3 cm^2 mol^{-1}	$10^{44}R$, esu^2 cm^2	freq, cm^{-1}	$10^{44}R$, esu^2 cm^2	assignment[e]
3054		0.35	1.54	3085	1.31	CH str, A′ out-of-phase
3041	31.7	−1.33	−3.23	3071	−2.99	CH str, A′ in-phase
3025		0.70	1.84	3060	1.69	CH str, A″
2271		0.31	1.32	2270	1.71	CD str, A′ in-phase
2258	14.2	−0.51	−2.14	2263	−2.36	CD str, A′ out-of-phase
2245		0.11	0.65	2251	0.69	CD str, A″
1348	4.1			1362		CHD scissors, A′ in-phase
1302	4.8			1305		CHD scissors, A″
1290	6.4			1295		CHD scissors, A′ out-of-phase
1163	3.1			1170		CHD twist + rock, A′ in-phase
1074	22.3			1081		CHD twist, A″
				1076		CHD wag, A″
1037	14.1			1040		CHD twist, A′ out-of-phase

[a] 0.017 M in C_2Cl_4 solution for CH and CD stretches; 0.017 M in CS_2 solution for mid-infrared; 0.8-cm path length; rotational strengths obtained from Lorentzian curve fits. [b] Frequencies calculated with empirical force field; rotational strengths calculated with coupled-oscillator model. [c] Calculated frequencies for modes below 1000 cm^{-1}: 937, 910, 869, 822, 750, 686, 602, 587 cm^{-1}. [d] Calculated frequencies for corresponding modes in *anti*-cyclopropane-*1*,*2*,*3*-$^{2}H_3$: 3087, 3072, 3067, 2272, 2263, 2263, 1368, 1308, 1296, 1176, 1081, 1083, 1042, 942, 920, 878, 825, 752, 687, 602, 587 cm^{-1}. [e] A′ and A″ refer to the symmetry species of the parent *anti*-cyclopropane-*1*,*2*,*3*-$^{2}H_3$ modes; in- and out-of-phase denote the relative phases of the motions at C(3) compared to those at C(1) and C(2). The largest contributions from ring stretch are at 1362, 1170, and 1040 cm^{-1}.

quency of a CD stretch, and a decrease of up to 20 cm^{-1} in the frequency of a ^{12}C–^{13}C stretch compared to a ^{12}C–^{12}C stretch. In this case, modes involving ^{12}CH and ^{13}CH stretches or bends will not be uncoupled, but the contributions to the normal modes from ^{12}CH and ^{13}CH will differ. For chiral ^{13}C substitution, all the vibrational modes could give rise to VCD signals.

The novel quadruply labeled chiral compound (2*S*,3*S*)-cyclopropane-*1*-^{13}C,^{2}H-*2*,*3*-$^{2}H_2$ (**1**) is derived from the achiral *anti*-cyclopropane-*1*,*2*,*3*-$^{2}H_3$ (**2**) by ^{13}C isotopic substitution at carbon 1. This molecule was of interest to us for the determination of

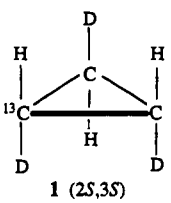

1 (2*S*,3*S*)

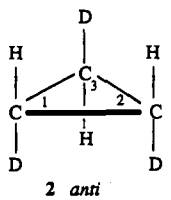

2 *anti*

the relative importance of one-center and two-center epimerization of cyclopropane through a study of the thermal stereomutations of **1**, as reported elsewhere.[14] That study depended on the measurement, using VCD spectroscopy, of the loss of optical activity during thermolysis of a sample of **1**. Sufficient VCD intensity for the analytical measurement was detected for a gas-phase sample in the CH stretching region, but not in other spectral regions.

In this report, we present a more complete study of the solution- and gas-phase VCD spectra of **1**. To our knowledge, this is the first molecule with chirality arising from ^{13}C substitution, or any isotopic substitution other than deuterium, to be investigated by a study of its vibrational optical activity. An interpretation of the sign and magnitude of VCD signals for the various normal modes of **1** is presented on the basis of a comparison of the calculated normal modes of **1** and **2** and a consideration of coupled-oscillator contributions.

Experimental Section

Samples of (2*S*,3*S*)-cyclopropane-*1*-^{13}C,^{2}H-*2*,*3*-$^{2}H_2$, (2*R*,3*R*)-cyclopropane-*1*-^{13}C,^{2}H-*2*,*3*-$^{2}H_2$, and the corresponding racemic quadruply labeled compound were prepared as previously described.[14,15] For the gas-phase studies, ~4-mg samples were transferred to a 5 cm path length Pyrex cell of ~20-mL volume, equipped with KBr windows, a high-vacuum stopcock, and a cold finger. For the solution-phase studies, a vacuum-tight Pyrex cell of 0.8-cm path length was constructed, with 25 mm diameter BaF_2 windows attached to the cell with Torr Seal and a side arm for condensing solvent and sample. Sample concentrations were accurately determined by condensing both sample and solvent from a known volume on a vacuum line, with pressures measured by a 1000-Torr high-accuracy Baratron gauge (MKS Instruments, Andover, MA) to ±0.1 Torr. For the CH and CD stretching regions, samples 0.017 M in C_2Cl_4 were used. Samples 0.017 M in CS_2 were examined in the CH stretching and 925–1375-cm^{-1} regions, which are free of intense solvent absorptions.

The VCD spectra in the CH and CD stretching regions were recorded on the dispersive VCD spectrometer previously described,[16] which was recently interfaced to an IBM XT computer with a Data Translation 2811 data acquisition board. Software for spectral scanning and data acquisition were written in Array Basic programming language for direct input into Spectra Calc (Galactic Industries, Salem, NH) for data manipulation and display. Two scans were recorded for each enantiomer at 8-cm^{-1} resolution and averaged, resulting in a noise level of 1×10^{-6} in absorbance. The VCD spectra in the mid-infrared region were recorded at 4 cm^{-1} on a modified Nicolet 7199 FTIR–VCD spectrometer,[17] with 12288 scans for each enantiomer; the noise level obtained was $(2.5–5) \times 10^{-6}$ in absorbance. Absorption spectra were measured with a Nicolet 7199 FTIR spectrometer at a nominal resolution of 8 cm^{-1} in the CH and CD stretching regions and 4 cm^{-1} in the mid-infrared region. The baseline-corrected spectra shown were obtained as half the difference in the raw VCD spectra obtained for the *S*,*S* and *R*,*R* enantiomers, with the exception of the gas-phase spectrum in the CD stretching region, which is the spectrum of the *S*,*S* enantiomer referenced to that of the racemic compound.

Lorentzian curve fitting and spectral simulations were carried out by using the Spectra Calc software.

Results

The VCD and absorption spectra of (2*S*,3*S*)-cyclopropane-*1*-^{13}C,^{2}H-*2*,*3*-$^{2}H_2$ in the CH and CD stretching regions for a gas-phase sample (83 Torr) and a sample 0.017 M in C_2Cl_4 solution are shown in Figure 1. Spectra obtained in the CH stretching region for a sample 0.017 M in CS_2 were nearly identical to those for the C_2Cl_4 solution sample. For the solution samples in both the CH and CD stretching regions, a (+,−,+) VCD sign pattern is observed; the VCD spectra are conservative, with approximately equal amounts of positive and negative intensity within each region. The mid-infrared absorption intensities of (2*S*,3*S*)-cyclopropane-*1*-^{13}C,^{2}H-*2*,*3*-$^{2}H_2$, 0.017 M in CS_2 solution, are compiled in Table I. No reproducible VCD signals were detected in this region for either the gas-phase or the solution sample. On the basis of the noise level in the VCD experiments, we estimate the upper limit for the anisotropy ratio for the more intense modes

(14) Cianciosi, S. J.; Ragunathan, N.; Freedman, T. B.; Nafie, L. A.; Lewis, D. K.; Glenar, D. A.; Baldwin, J. E. *J. Am. Chem. Soc.* **1991**, *113*, 1864.

(15) Cianciosi, S. J. Ph.D. Dissertation, Syracuse University, 1990.

(16) (a) Diem, M.; Gotkin, P. J.; Kupfer, J. M.; Tindall, A. G.; Nafie, L. A. *J. Am. Chem. Soc.* **1977**, *99*, 8103. (b) Diem, M.; Gotkin, P. J.; Kupfer, J. M.; Nafie, L. A. *J. Am. Chem. Soc.* **1978**, *100*, 5644. (c) Diem, M.; Photos, E.; Khouri, H.; Nafie, L. A. *J. Am. Chem. Soc.* **1979**, *101*, 6829.

(17) Lipp, E. D.; Nafie, L. A. *Appl. Spectrosc.* **1984**, *38*, 20.

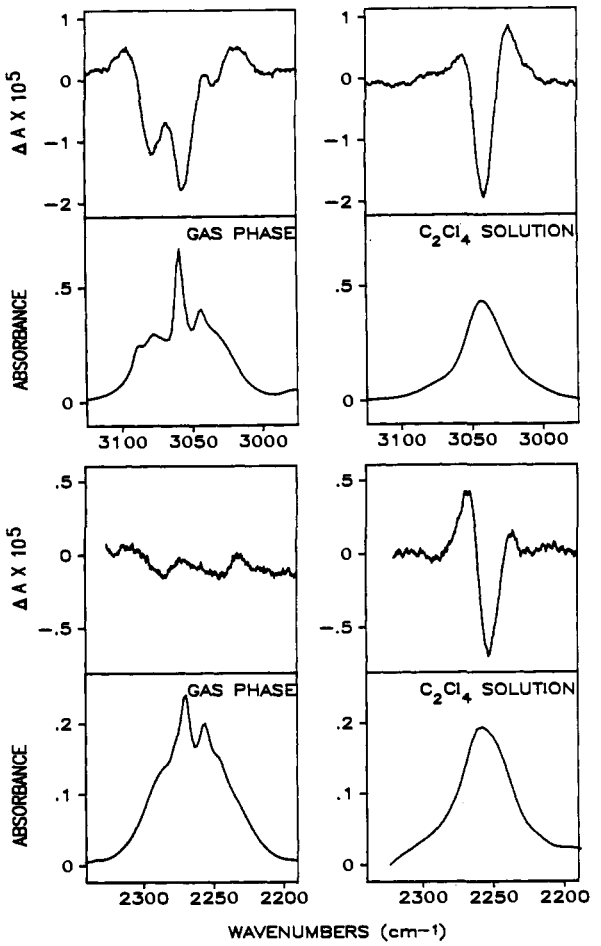

Figure 1. Absorption (lower traces) and VCD (upper traces) spectra of (2*S*,3*S*)-cyclopropane-*1*-^{13}C,^{2}H-*2*,*3*-$^{2}H_2$ in the CH and CD stretching regions. Gas-phase samples: 83 Torr, 5-cm path length. Solution samples: 0.017 M in C_2Cl_4, 0.8-cm path length.

at 1074 and 1037 cm^{-1} to be 2×10^{-5}. There was insufficient sample available to detect any VCD signals for the bands between 1100 and 1375 cm^{-1} with anisotropy ratios below $\sim 1 \times 10^{-4}$. On the basis of the comparisons with the VCD spectra in this region that we have recorded for (*S*,*S*)-cyclopropane-*1*,*2*-$^{2}H_2$,[18] we conclude that any VCD signals for **1** in this region must be at least 5–10 times weaker than those for (*S*,*S*)-cyclopropane-*1*,*2*-$^{2}H_2$.

Frequencies and assignments are presented in Table I. The band assignments for the observed modes are derived from the calculated Cartesian displacement derivatives (vide infra) and comparisons of the corresponding modes of **1** and **2** (see Figure 2); in Table I, each mode for **1** is described by the symmetry species (A′, symmetric to reflection across the plane of symmetry; A″, antisymmetric to reflection) and phasing of the mode for **2** from which it is derived.

Interpretation and Calculations

In order to understand the origin of the VCD signals in **1**, normal-coordinate calculations for **1** and **2** were carried out by employing the empirical force field for cyclopropane of Duncan and Burns,[19] transferred to internal coordinates.[20] This force field gives mid-infrared frequencies that agree with experiment for both **1** and (*S*,*S*)-cyclopropane-*1*,*2*-$^{2}H_2$ (**3**).[5,18] However, in the CH stretching region, the calculated frequency ordering for the two modes of **3** involving in- and out-of-phase C(1)H and C(2)H stretches is opposite to that observed. To bring the calculated frequencies and mode assignments into better agreement with

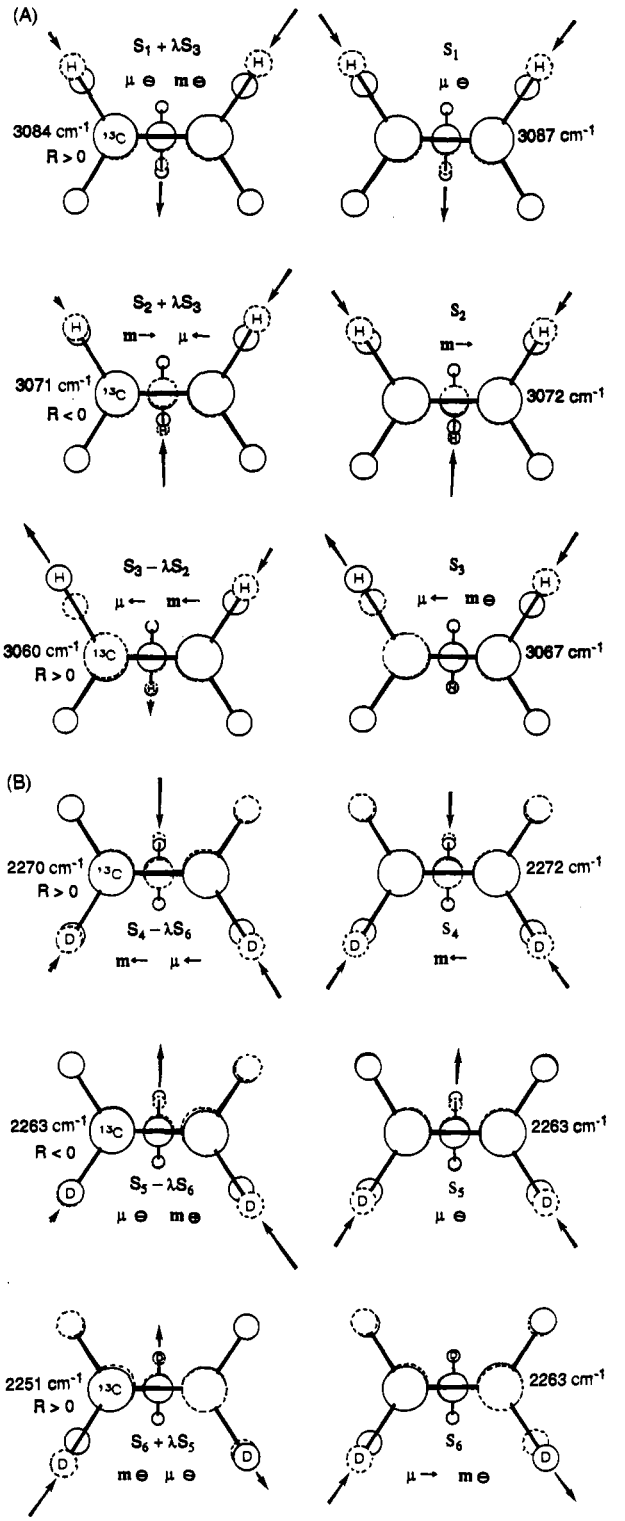

Figure 2. Schematic representations of the calculated normal modes of (2*S*,3*S*)-cyclopropane-*1*-^{13}C,^{2}H-*2*,*3*-$^{2}H_2$ in the (A) CH stretching and (B) CD stretching regions, compared with the corresponding modes of *anti*-cyclopropane-*1*,*2*,*3*-$^{2}H_3$ on the right. The dotted and solid circles represent the two extremes of the vibrational cycle; the arrows indicate the relative directions and magnitudes of the local electric dipole transition moments arising from CH or CD motion. For *anti*-cyclopropane-*1*,*2*,*3*-$^{2}H_3$, the modes at 3067 and 2263 cm^{-1} have A″ symmetry and the other four have A′ symmetry. For each mode of **2** on the right, the direction of the net positive electric dipole transition moment μ and the direction of the magnetic dipole transition moment **m**, deduced from the sense of circulation of the local electric moments, are shown. The modes of **1** on the left are decomposed into linear combinations of modes S_1–S_6 on the right (where λ is a small mixing parameter), and the directions of the relevant μ and **m** contributions are indicated.

(18) Freedman, T. B.; Spencer, K. M.; Cianciosi, S. J.; Ragunathan, N.; Baldwin, J. E. Manuscript in preparation.
(19) Duncan, J. L.; Burns, G. R. *J. Mol. Spectrosc.* **1969**, *30*, 253.
(20) Lowe, M. A.; Segal, G. A.; Stephens, P. J. *J. Am. Chem. Soc.* **1986**, *108*, 256.

experiment for the CH stretches, the interaction force constant for anti CH bond stretches[20] was increased from −0.0033 to −0.015 mdyn/Å.

From the schematic comparison of the calculated CH and CD stretching normal modes of **1** and **2** shown in Figure 2, it is evident that the chiral ^{13}C substitution, with a concomitant decrease in vibrational frequency for the ^{13}CH (or ^{13}CD) stretch relative to the other two CH (or CD) stretches, has removed the reflection symmetry of the modes, slightly mixing A′ and A″ character while maintaining the relative phases of the oscillators.

We consider two approaches to understanding the effect of the chiral perturbation from the ^{13}C substitution in producing the observed VCD bands. VCD intensity is proportional to the rotational strength, the scalar product of the electric dipole transition moment μ and the magetic dipole transition moment **m**. Qualitatively, VCD intensity is the result of the simultaneous occurrence during the vibration of angular charge oscillation (which gives rise to a magnetic dipole transition moment, **m**) about the direction of linear charge oscillation (which gives rise to an electric dipole transition moment, μ). For the modes of **2** shown on the right in Figure 2, we can consider the arrows to represent local electric dipole transition moments arising from the individual bond stretches or contractions. The vector sum of the arrows gives the direction of positive linear charge motion for the phase of oscillation shown. The sense of circulation, if any, of the arrows about the center of mass leads to the direction of the magnetic dipole transition moment by application of the right-hand rule for positive charge circulation. With this interpretation, modes S_1 and S_5 have a large contribution from linear charge motion into the plane of the figure, and modes S_2 and S_4 have a large contribution from angular charge motion about the center of mass that corresponds to a magnetic dipole transition moment directed to the right for S_2 and to the left for S_4. The angular charge motion in either S_3 or S_6 results in a magnetic dipole transition moment into the plane of the figure; the net electric dipole transition moment is directed to the left for S_3 and to the right for S_6. For each mode of the achiral molecule **2**, either μ and **m** are orthogonal or one transition moment is zero; no VCD intensity is possible. The perturbation by ^{13}C substitution results in modes of **1** that can be decomposed into linear combinations of the A′ and A″ modes of **2**, as shown on the left in Figure 2. As a consequence of this admixture, the linear and angular charge motion in the modes of **1** give rise to electric dipole and magnetic dipole transition moments that have parallel or antiparallel components. The signs of the rotational strengths (denoted *R* in Figure 2) predicted by this interpretation agree in all cases with those experimentally observed.

The spectra can also be interpreted in an alternative qualitative manner. The in- and out-of-phase coupled vibrations of pairs of chirally oriented local oscillators give rise to VCD signals via the coupled oscillator mechanism.[21-25] The signs and magnitudes of the VCD signals in **1** can be understood by considering the relative contributions to each mode from the two pairs of coupled, chirally oriented trans CH or CD oscillators. For example, for the mode calculated at 3084 cm^{-1} (Figure 2), the local electric dipole transition moments for the pair of trans CH oscillators on carbons 2 and 3, which are oriented and phased to produce positive coupled-oscillator VCD signals, make a larger contribution to the mode than the electric dipole transition moments for the pair of trans CH oscillators on carbons 1 and 3, which are phased and oriented to produce negative VCD signals. Thus, a net positive VCD signal is predicted, as observed. In general, for the CH or CD stretching modes of **1** deriving from the A′ modes in **2**, the VCD signal arises from unequal contributions of opposite sign from the two pairs of trans oscillators. For the modes of **1** deriving from the A″ modes in **2**, the VCD signals arise from small contributions from C(3)H or C(3)D displacement in the C(3)HD plane, which are forbidden by symmetry in **2**, but which can mix with the displacements at C(1) and C(2) when the symmetry is lowered by ^{13}C substitution. VCD intensity contributions of the same sign arise from the two coupled oscillators formed by these small displacements at C(3) and the displacement at C(1) or C(2).

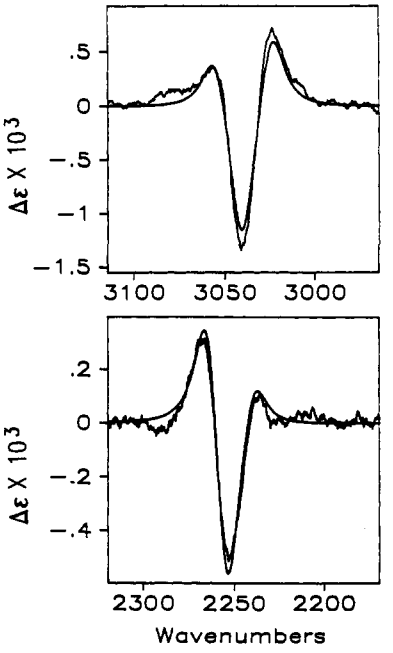

Figure 3. Comparison of the observed VCD spectra of (2*S*,3*S*)-cyclopropane-*1*-^{13}C,^{2}H-*2*,*3*-$^{2}H_2$ in the CH and CD stretching regions with spectra calculated by using the generalized coupled-oscillator model and an empirical force field normal-coordinate calculation.

A quantitative application of the coupled-oscillator model to the CH and CD stretching VCD spectra of **1** can be made by using the relative Cartesian displacements determined by the normal-coordinate calculation to write normalized approximate normal modes of the form

$$\mathcal{L}_i = a_{i1}\Delta(\mathrm{C(1)H}) + a_{i2}\Delta(\mathrm{C(2)H}) + a_{i3}\Delta(\mathrm{C(3)H}) \quad (1)$$

for the CH stretches and analogous expressions for the CD stretches involving only the displacements of the CD bonds. The rotational strength of the *i*th mode is determined from the generalized coupled-oscillator expression for nonchiral identical oscillators (derived in the Appendix)

$$R_i = -\pi\nu_i\frac{D_T}{N}\sum_{k>j}^{N} a_{ij}a_{ik}\mathbf{R}_{jk}\cdot\hat{\mathbf{u}}_j\times\hat{\mathbf{u}}_k \quad (2)$$

where ν_i is the frequency (cm^{-1}) of the *i*th mode, D_T is the total dipole strength obtained by integrating the area under the experimental absorption bands giving rise to the VCD, *N* is the number of CH or CD oscillators, and $\mathbf{R}_{jk}$ is the $j \rightarrow k$ separation vector between a pair of oscillators *j* and *k*, which have unit vectors $\hat{\mathbf{u}}_j$ and $\hat{\mathbf{u}}_k$, located on the corresponding bond and directed C → H or C → D. The oscillators have individual contributions a_{ij} and a_{ik} to the approximate normal mode. The summation is over all pairs of chirally oriented oscillators. This model ignores any charge flow between local oscillators during the coupled vibrations[26,27] and assumes that the electric dipole moment changes lie along the bond directions. Under these conditions, the separation vector $\mathbf{R}_{jk}$ can connect any two points along the bond axes of the two oscillators (see Appendix). The small difference in dipole strength for the ^{13}CH or ^{13}CD stretch compared to the ^{12}CH or ^{12}CD stretch is also ignored.

The results of the application of this model to the CH and CD stretching VCD spectra of **1** are shown in Table I and Figure 3.

(21) Holzwarth, G.; Chabay, I. *J. Chem. Phys.* **1972**, *57*, 1632.
(22) Tinoco, I. *Radiat. Res.* **1963**, *20*, 133.
(23) Gulotta, M.; Goss, D. J.; Diem, M. *Biopolymers* **1989**, *28*, 2047.
(24) Sugeta, H.; Marcott, C.; Faulkner, T. R.; Overend, J.; Moscowitz, A. *Chem. Phys. Lett.* **1976**, *40*, 397.
(25) Faulkner, T. R. Ph.D. Dissertation, University of Minnesota, 1976.
(26) Polavarapu, P. L. *J. Chem. Phys.* **1987**, *87*, 4419.
(27) Polavarapu, P. L.; Bose, P. K. *Chem. Phys. Lett.* **1988**, *143*, 337.

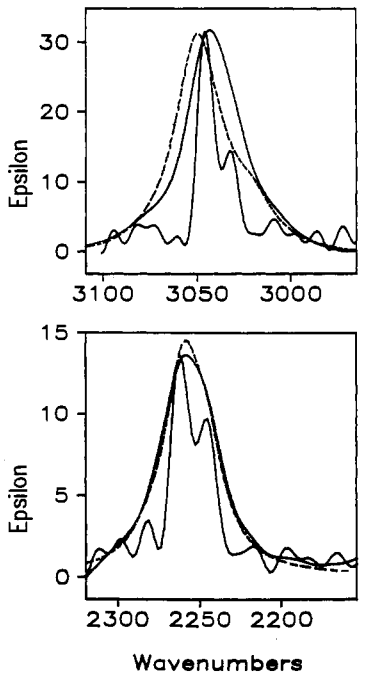

Figure 4. Comparison of the observed absorption spectra (—) of (2*S*,3*S*)-cyclopropane-*1*-^{13}C,^{2}H-*2*,*3*-$^{2}H_2$ in the CH and CD stretching regions and the calculated spectra (---) obtained from the coupled-oscillator modes used to generate the simulated VCD spectra in Figure 3. Also shown, with a compressed ordinate scale, are Fourier deconvolutions of the observed absorption spectra.

The dipole strength per oscillator obtained from the absorption band areas is 1.40×10^{-39} esu^2 cm^2 for the CH stretches and 1.05×10^{-39} esu^2 cm^2 for the CD stretches; the ratio of these values is close to 1.363, the intensity ratio for isolated CH and CD diatomic harmonic oscillators ($I_{CH}/I_{CD} = (\mu_{CD}/\mu_{CH})^{1/2}$, where μ is the reduced mass of the diatomic oscillator). In Table I, we compare the calculated coupled-oscillator rotational strengths with the rotational strengths determined from Lorentzian curve fits to the observed VCD spectra. The latter represent a lower limit to the actual experimental rotational strengths, since somewhat more intense bands with more extensive cancellation from overlap could also fit the observed VCD spectrum within the experimental error for the band shapes. For Figure 3, the calculated VCD intensities were converted to Lorentzian bands having the average band width determined from the Lorentzian fit to the observed VCD data; the frequencies of the calculated bands were adjusted for best fit to the observed spectra. The latter procedure resulted in an increase of $\sim$1–5 cm^{-1} in the separation of adjacent bands compared to the calculated frequency separations. It is clear that the observed VCD intensities are explained quite well by this simple model. Figure 4 includes a comparison of the observed absorption spectra with those simulated from the set of modes generated by the local oscillators, which gave rise to the VCD simulation in Figure 3. Also shown in Figure 4 is the Fourier deconvolution of the observed absorption spectrum. The local-oscillator description of the CH stretching modes results in a {strong, very weak, medium} absorption intensity pattern, from high to low frequency, in agreement with the Fourier deconvolution of the observed spectrum. The discrepancy in the band contours for the observed and simulated spectra indicates that the frequency separation of the modes in the calculated spectrum is too large in this region. In the CD stretching region, the observed and calculated absorption band contours agree closely, and the {weak, strong, medium} intensity pattern calculated for the three modes is consistent with the Fourier deconvolution of the observed absorption spectrum.

Discussion

The results of this investigation demonstrate that chirality introduced by ^{13}C substitution can produce observable VCD intensity for CH and CD stretching modes. In the case examined here, the symmetry lowering alters the coupling between chirally oriented oscillators. The perturbations of the modes from the symmetric parent molecule are large in the CH and CD stretching regions, and the modes within each region are fairly well separated in frequency. These VCD bands with anisotropy ratios on the order of 5×10^{-5} were readily observed. In the mid-infrared region, the deviations from A′ and A″ symmetry are not as large; each mode involves both H and D displacements, and ring stretching as well. Thus, we might expect the VCD intensities in the mid-infrared region to be weaker. Although we were unable to observe VCD intensity in the mid-infrared region, our noise levels in that region were 2–5 times larger than those obtainable with the dispersive VCD instrument, and insufficient sample was available to increase the absorbances of the bands. However, comparison of the spectral intensities in corresponding regions for **1** and (*S*,*S*)-cyclopropane-*1*,*2*-$^{2}H_2$ does suggest that the effects of the chiral substitution are less for the mid-infrared vibrations.

In the CD stretching region, no significant VCD intensity was observed for the gas-phase sample, in contrast to the weak but distinct VCD observed for the solution sample. In the gas phase, the bands are considerably broadened due to coupling with rotational transitions, and the oppositely signed VCD signals from adjacent vibrational modes apparently cancel. As is evident from the absorption spectra, the vibrational modes for the gas-phase sample are more widely separated in the CH stretching region, and less cancellation occurs.

The qualitative interpretation of the VCD spectra of **1** in terms of the chiral perturbation of modes of a parent, achiral molecule is a method that has also been successfully applied to the interpretation of the VCD spectra of (*S*,*S*)-cyclopropane-*1*,*2*-$^{2}H_2$[18] and (*S*,*S*)-oxirane-*2*,*3*-$^{2}H_2$.[28] For this set of molecules, a description of the modes in terms of local electric dipole moment contributions is sufficient for understanding the signs of the observed VCD bands; no consideration of additional intrinsic magnetic effects is required.

The earliest formulation of the coupled-oscillator mechanism for VCD considered only the case of two degenerate achiral oscillators,[21] for which the product of coefficients in eq 2 is $\pm^1/_2$. The formulation of the model has been extended to include a pair of nondegenerate oscillators,[25] more than two oscillators,[23,29] and a pair of identical chiral oscillators with intrinsic magnetic dipole moments.[24] Most of the applications of the model have involved either a single pair of oscillators or a set of oscillators coupled via a dipolar interaction potential.[22,23,30] In the latter case, the coefficients in eq 2 are determined by solving a secular determinant for a perturbed set of degenerate oscillators,[23] although for symmetrically disposed oscillators (e.g. three oscillators interchanged by a C_3 axis), the coefficients are more readily determined from group theory.[30] The current study provides a more general formulation of the coupled-oscillator model for achiral oscillators, one that has not been previously presented. This formulation encompasses the previous applications and also includes the case for which the relative contributions from coupled oscillators in a molecule lacking symmetry are determined from the normal-coordinate analysis. The expression in eq 2 could also be readily extended to the case of nonidentical coupled oscillators with different intrinsic dipole strengths by replacing D_T/N with the product $D_j^{1/2}D_k^{1/2}$ for each pair of oscillators j and k, if these individual dipole strengths for the local oscillators can be independently measured from specific isotopomers. In these respects, this generalized coupled-oscillator model resembles the fixed partial charge (FPC) model,[31] which treats the displacement of each individual atom but which requires an additional parametrization

(28) Freedman, T. B.; Spencer, K. M.; Ragunathan, N.; Nafie, L. A.; Moore, J. A.; Schwab, J. M. *Can. J. Chem.*, in press.
(29) Schellman, J. A. In *Peptides, Polypeptides and Proteins*; Blout, E. R., Vobey, F. A., Goodman, M., Lotan, N., Eds.; Wiley: New York, 1974; pp 320–337.
(30) Paterlini, M. G.; Freedman, T. B.; Nafie, L. A.; Tor, Y.; Shanzer, A. Manuscript in preparation.
(31) Schellman, J. A. *J. Chem. Phys.* **1973**, *58*, 2882; **1974**, *60*, 343.

to assign fixed partial charges that best reproduce the dipole strengths.

In order to obtain a fit to the observed VCD spectra by using the generalized coupled-oscillator model, a single force constant was altered from the empirical force field derived from the gas-phase vibrational spectra of cyclopropane and cyclopropane-d_6.[19,20] The anti CH/CH stretching interaction force constant affects the extent and phasing of the coupling between trans CH stretches. With the original value of this force constant, the VCD patterns in the CH and CD stretching regions of **1** were reproduced, but the predicted intensities in the CH stretching region were too small, and those in the CD stretching region too large. Increasing the magnitude of this force constant increased the admixture of A′ and A″ character for the CH stretches and brought the calculation into agreement with experiment. The same final value for this force constant corrected two areas of disagreement between calculation and experiment for the VCD spectra of (*S,S*)-cyclopropane-*1,2*-$^2H_2$: an incorrect frequency ordering for the in- and out-of-phase trans CH stretches at carbons 1 and 2 and incorrect magnitudes for the VCD intensities for the bands arising primarily from the antisymmetric and symmetric CH_2 stretches.[5,18] The difference in band contours between the observed and calculated CH stretching absorption spectra of **1** (Figure 4) suggests that the VCD spectrum results from individual contributions that are larger than calculated but are closer together in frequency and thus undergo more extensive cancellation. We find that decreasing the syn CH/CH stretching force constant in the original empirical force field has the desired effect of increasing the magnitudes of the coupled-oscillator VCD intensities while decreasing the separation between CH stretching modes. However, we are not aiming to fit a force field based on a simplified intensity model, and we have chosen here to make an adjustment in only a single force constant that results in the correct mode assignment for (*S,S*)-cyclopropane-*1,2*-$^2H_2$.

The excellent agreement between experiment and calculation for the generalized couupled-oscillator model indicates that the coupled-oscillator mechanism provides a valid and valuable description of the origin of VCD intensity, when the modes can be attributed to the coupled oscillation of chirally oriented oscillators, and the VCD spectra in the region of coupling are basically conservative. The agreement with experiment in this case also depends on the fact that charge flow is largely confined within the oscillator for this hydrocarbon. However, if properly applied, even when this restriction does not hold (as long as one phase of the coupled motion does not produce considerably more extended charge flow in the molecule compared to the other phase or phases), the coupled-oscillator mechanism can provide valid interpretations of VCD spectra and descriptions of molecular conformation deduced from VCD patterns. As a result of the findings presented in this paper, we do not agree with the point of view offered elsewhere[32] that applications of the coupled-oscillator model "do not provide a sound basis for prediction and analysis of VCD spectra" and that past and future applications of this model are unwarranted. These opinions were apparently based in part on a few comparisons of ab initio and coupled-oscillator calculations which have been only partially compared on a quantitative basis to experiment.[32] Stephens et al.[32,35] have deduced the *form* of the coupled-oscillator model from the **P·L** (atomic polar tensor model[33,34]) contribution to his distributed origin gauge, magnetic field perturbation expressions. The conclusion in that work[32] is that the coupled-oscillator model is a further, lower accuracy approximation to the atomic polar tensor (APT) equations[33,34] and that the coupled-oscillator model can therefore be discounted since the APT equations do not accurately predict VCD intensities. In the magnetic dipole transition moment contributions to the APT model, however, the change in the *total* molecular dipole moment due to the motion of a nucleus is located at that moving nucleus. Our alternative derivation of the coupled-oscillator model, presented in the Appendix, is based on local dipole moment contributions and suggests that the **P·M** term of Stephens[35] (which is ignored in his derivation of the form of the coupled-oscillator model) contains corrections to the location of local contributions in addition to more intrinsic magnetic effects. The *form* of the coupled-oscillator equations is, in fact, the only one consistent with the restrictions of the model, and one need not carry out a detailed derivation from rigorous theory to deduce that form. We further note that it is precisely for those vibrational modes that involve isolated local coupled oscillations that the FPC model (and in some cases the APT model) provides adequate calculated VCD intensities, particularly for CH stretching modes.[18,20,36-38] Certainly, the coupled-oscillator model should not be employed with impunity. There are numerous cases of isolated local vibrational motion that produces large VCD intensity in the absence of nuclear vibrational coupling, intensity that must derive from intrinsic magnetic dipole moment effects. However, for the global understanding of VCD intensity, a mechanism involving electric dipole moments in a chiral geometric arrangement remains an important and valuable interpretational tool.

The use of chirality introduced by ^{13}C substitution is promising for future studies of reaction mechanisms in which VCD can be used to follow reaction kinetics in nonderivatized hydrocarbons. This study indicates that this chiral substitution must be made in a manner which alters the coupling among chirally oriented CH or CD oscillators.

Acknowledgment. We acknowledge support of this work by grants from the National Institutes of Health (GM-23567) to T.B.F. and L.A.N. and from the National Science Foundation (CHE-87-21656) to J.E.B.

Appendix

Vibrational circular dichroism intensity is proportional to the rotational strength, the scalar product of the electric dipole and magnetic dipole transition moments. With the velocity formulation of the electric dipole moment operator, the rotational strength of a fundamental transition for the ith normal mode at angular frequency ω_i is given by[39]

$$R_i(0\rightarrow 1) = \omega_i^{-1}\ \mathrm{Re}\ [(\mu_v)_{01}\cdot(\mathbf{m})_{10}] \qquad \text{(A1)}$$

The components of the electric dipole transition moment can be expressed in terms of the velocity form of the atomic polar tensor (APT), $P^{A}_{v,\alpha\beta}$, and the Cartesian displacement derivative for atom A in the ith normal mode, $s_{A\alpha,i}$

$$(\mu_{v,\beta})_{01} = -i\left(\frac{\hbar\omega_i}{2}\right)^{1/2}\sum_{A} P^{A}_{v,\alpha\beta}s_{A\alpha,i} \qquad \text{(A2)}$$

In this and following expressions, summation over repeated Greek subscripts is implied. The APT is the derivative of the current density with respect to the velocity $\dot{\mathbf{R}}_A$ of nucleus A at the collective nuclear positions **R**, evaluated at the equilibrium nuclear positions and zero nuclear velocities (denoted by subscripts 0,0)[40,41]

$$P^{A}_{v,\alpha\beta} = \left(\frac{\partial}{\partial\dot{R}_{A\alpha}}\int j_\beta(\mathbf{r},\mathbf{R},\dot{\mathbf{R}})\ d\tau\right)_{0,0} \qquad \text{(A3)}$$

The components of the magnetic dipole transition moment can

(32) Stephens, P. J.; Jalkanen, K. J.; Kawiecki, R. W. *J. Am. Chem. Soc.* **1990**, *112*, 6518.
(33) Freedman, T. B.; Nafie, L. A. *J. Chem. Phys.* **1983**, *78*, 27; **1983**, *79*, 1104.
(34) Freedman, T. B.; Nafie, L. A. *J. Phys. Chem.* **1984**, *88*, 496.
(35) Stephens, P. J. *J. Phys. Chem.* **1987**, *91*, 1712.
(36) Freedman, T. B.; Kallmerten, J.; Lipp, E. D.; Young, D. A.; Nafie, L. A. *J. Am. Chem. Soc.* **1988**, *110*, 698.
(37) Annamalai, A.; Keiderling, T. A.; Chickos, J. S. *J. Am. Chem. Soc.* **1984**, *106*, 6254.
(38) Annamalai, A.; Jalkanen, K. J.; Narayanan, U.; Tissot, M.-C.; Keiderling, T. A.; Stephens, P. J. *J. Phys. Chem.* **1990**, *94*, 194.
(39) Hansen, A. E.; Bouman, T. D. In *Advances in Chemical Physics*; Prigogine, I., Rice, S. A., Eds.; Wiley: New York, 1980; Vol. 44, p 545.
(40) Nafie, L. A. *J. Chem. Phys.* **1983**, *79*, 4950.
(41) Nafie, L. A.; Freedman, T. B. *J. Phys. Chem.* **1986**, *90*, 763.

be expressed in terms of the atomic axial tensor (AAT) $M^{A}_{\alpha\beta}$[35,42,43]

$$(m_\beta)_{10} = i\left(\frac{\hbar\omega_i}{2}\right)^{1/2}\sum_A M^A_{\alpha\beta}s_{A\alpha,i} \quad \text{(A4)}$$

The AAT is the derivative of the angular current density with respect to the velocity of nucleus A[40,41]

$$M^A_{\alpha\beta} = \left(\frac{\partial}{\partial \dot{R}_{A\alpha}}\frac{1}{2c}\int \epsilon_{\beta\gamma\delta}r_\gamma j_\delta(\mathbf{r},\mathbf{R},\dot{\mathbf{R}})\,d\tau\right)_{0,0} \quad \text{(A5)}$$

where $\epsilon_{\beta\gamma\delta}$ is the unit antisymmetric tensor. The local nature of the contributions to the AAT is clear from this expression: the moment arm r is directed to the element of the current density j located at position r.

When expressed explicitly in terms of atomic orbitals and electronic operators acting on those orbitals,[42,43] each APT and AAT can be further broken down into atomic contributions, which we denote respectively as $[P^A_{v,\alpha\beta}]^B$ and $[M^A_{\alpha\beta}]^B$ for the contribution from atom B to the $\alpha\beta$ component of the APT and AAT for atom A. The electronic contribution for atom B is uniquely defined by summing all the terms for which the electronic momentum operator or angular momentum operator acts on an orbital belonging to atom B. The nuclear contribution is part of $[P^A_{v,\alpha\beta}]^A$ or $[M^A_{\alpha\beta}]^A$. When the electronic contributions to the velocity form of the APT and the AAT are expressed in terms of atomic orbitals with electric dipole vector potential perturbation[44] and external magnetic field perturbation,[45] respectively, a similar breakdown into atomic contributions for atom B can be made by summing over all the terms for which the field perturbation derivative acts on a coefficient of an orbital of atom B.[44,45]

The APT is written as a sum of the contributions from all the atoms

$$P^A_{v,\alpha\beta} = \sum_B [P^A_{v,\alpha\beta}]^B \quad \text{(A6)}$$

The form of the AAT suitable for evaluation in terms of molecular orbitals depends on the choice of origin for the magnetic dipole moment operator. In the common origin (CO) gauge,[35] a common molecular origin is chosen for all atomic contributions; the AAT can be expressed as a sum of the atomic contributions

$$(M^A_{\alpha\beta})^{CO} = \sum_B [(M^A_{\alpha\beta})^{CO}]^B \quad \text{(A7)}$$

We use parentheses followed by a superscript to denote the origin for the magnetic dipole moment operator and square brackets followed by a superscript to denote an atomic contribution.

The origin for the magnetic dipole moment operator for each atom can also be chosen to be the moving atom A. In this distributed origin (DO) gauge,[35] the AAT reduces to a term with a moment arm from the molecular origin to atom A crossed into the APT for atom A, plus an AAT with the origin at atom A:

$$\begin{aligned}(M^A_{\alpha\beta})^{DO} &= \frac{1}{2c}\epsilon_{\beta\gamma\delta}R^0_{A\gamma}\sum_B [P^A_{v,\alpha\delta}]^B + \sum_B [(M^A_{\alpha\beta})^A]^B \\ &= \frac{1}{2c}\epsilon_{\beta\gamma\delta}R^0_{A\gamma}P^A_{v,\alpha\delta} + (M^A_{\alpha\beta})^A \end{aligned} \quad \text{(A8)}$$

The first term in eq A8 is the magnetic dipole moment portion of the atomic polar tensor model for VCD, which leads to the "**P**·**L** term" of Stephens; the second term leads to the "**P**·**M** term" of Stephens.[35]

We consider here a third choice of origin, which we call the locally distributed origin (LDO), where for the individual atomic contribution from atom B, the origin for the magnetic dipole moment operator is placed at the atomic center for atom B. In this case, the AAT reduces to a summation involving a moment arm to each atom B crossed into the contribution from that atom to the APT, plus a summation over intrinsic contributions for atom B with origin at B:[42,43]

$$(M^A_{\alpha\beta})^{LDO} = \sum_B \frac{1}{2c}\epsilon_{\beta\gamma\delta}R^0_{B\gamma}[P^A_{v,\alpha\delta}]^B + \sum_B [(M^A_{\alpha\beta})^B]^B \quad \text{(A9)}$$

In this expression, B is in general different from atom A. The intrinsic contributions consist of one- and two-center terms, to which only atom B and nearest-neighbor atoms whose orbitals overlap significantly with those of atom B make large contributions. This choice of origin retains the local nature of the contributions to the AAT implied in the general expression, eq A5. In contrast, in eq A8 the moment arm is directed to an APT for the whole molecule, and the second term of eq A8 depends on atom A for its origin and two other atomic orbital centers that can be far removed from A. This breakdown of the AAT is clearly nonlocal. We have previously shown that the second term in eq A8 contains corrections to the APT model.[34,42]

The expression for the rotational strength with locally distributed origins is

$$\begin{aligned}R_i(0\rightarrow 1) &= \frac{\hbar}{4c}[\sum_A\sum_B [P^A_{v,\alpha\beta}]^B s_{A,\alpha i}]\cdot[\sum_{A'}\sum_{B'}\{\epsilon_{\beta\gamma\delta}R^0_{B'\gamma}[P^{A'}_{v,\delta\gamma}]^{B'} + \\ &\qquad [(M^{A'}_{\alpha\beta})^{B'}]^{B'}\}s_{A'\delta,i}] \\ &= \frac{\hbar}{4c}\left[\sum_B\left(\frac{\partial\mu^B_v}{\partial P_i}\right)_0\right]\cdot\left[\sum_{B'}\left\{\mathbf{R}^0_B\times\left(\frac{\partial\mu^{B'}_v}{\partial P_i}\right)_0 + \left(\frac{\partial \mathbf{m}^{B'}_{loc}}{\partial P_i}\right)_0\right\}\right]\end{aligned} \quad \text{(A10)}$$

where the second line is in vector form, and P_i is the conjugate momentum for normal mode Q_i. Up to this point, no approximations have been invoked beyond those usually employed for a priori VCD calculations. An equation of the same form as eq A10 has been used previously without derivation to derive most models of VCD.[34]

We now consider a normal mode arising from the coupled motion of a set of N identical, achiral, isolated local oscillators. Each local oscillator, labeled j, consists of two atoms and has a local electric dipole transition moment along its bond axis for the bond-stretching motion. The normal mode can be written as $Q_i = \sum_j a_{ij}\Delta l_j$. The atomic contributions to the electric dipole moment derivatiove for the mode can be regrouped into local-oscillator contributions

$$\sum_B\left(\frac{\partial\mu^B_v}{\partial P_i}\right)_0 = \sum_j\sum_{B_j}\left(\frac{\partial\mu^{B_j,j}_v}{\partial P_i}\right)_0 = \sum_j\left(\frac{\partial\mu^j_v}{\partial P_i}\right)_0 \quad \text{(A11)}$$

where B_j is the sum over the two atoms in oscillator j. Since the local oscillators are achiral, we can ignore the intrinsic contributions to the magnetic dipole moment derivative. The coupled-oscillator rotational strength is

$$R_i(0\rightarrow 1) \cong \frac{\hbar}{4c}\left[\sum_j\left(\frac{\partial\mu^j_v}{\partial P_i}\right)_0\right]\cdot\left[\sum_{j'}\mathbf{R}^0_{j'}\times\left(\frac{\partial\mu^{j'}_v}{\partial P_i}\right)_0\right] \quad \text{(A12)}$$

where $\mathbf{R}^0_j$ can be directed to any point along the bond axis and $\mathbf{R}^0_{j'}$ can be the same for the two atoms in the oscillator, as shown below.

Since the oscillators are identical and isolated, we can write

$$\left(\frac{\partial\mu^i_v}{\partial P_i}\right)_0 = \left|\frac{\partial\mu^0}{\partial S}\right|\hat{\mu}a_{ij} \quad \text{(A13)}$$

where $|\partial\mu^0/\partial S|$ is the magnitude of the local electric dipole moment derivative and the unit vector $\hat{u}_j$ along the axis of oscillator j is directed toward positive dipole moment change. The rotational and dipole strengths reduce to

(42) Freedman, T. B.; Nafie, L. A. *J. Chem. Phys.* **1988**, *89*, 374.
(43) Nafie, L. A. *J. Chem. Phys.*, submitted for publication.
(44) Amos, R. D.; Jalkanen, K. J.; Stephens, P. J. *J. Phys. Chem.* **1988**, *92*, 5571.
(45) Amos, R. D.; Handy, N. C.; Jalkanen, K. J.; Stephens, P. J. *Chem. Phys. Lett.* **1987**, *133*, 21.

$$R_i(0\rightarrow 1) = \frac{\hbar}{4c}\left|\frac{\partial\mu_0}{\partial S}\right|^2 \sum_{j,j'}^{N} a_{ij}a_{ij'}\hat{\mu}_j \cdot \mathbf{R}_{j'}^0 \times \hat{\mu}_{j'} \qquad \text{(A14)}$$

$$D_i(0\rightarrow 1) = \frac{\hbar}{2\omega_i}\left|\frac{\partial\mu^0}{\partial S}\right|^2 \sum_{j,j'}^{N} a_{ij}a_{ij'}\hat{\mu}_j \cdot \hat{\mu}_{j'} \qquad \text{(A15)}$$

The total dipole strength for the N modes arising from the coupling of the set of oscillators is

$$D_T = \sum_{i=1}^{N} D_i(0\rightarrow 1) = \frac{\hbar N}{2\omega_i}\left|\frac{\partial\mu^0}{\partial S}\right|^2 \qquad \text{(A16)}$$

By substituting eq A16 into eq A14 and rearranging the triple product, we obtain the generalized coupled-oscillator expression for N nonchiral identical oscillators

$$R_i(0\rightarrow 1) = -\pi\nu_i \frac{D_T}{N}\sum_{j>j'}^{N} a_{ij}a_{ij'}\mathbf{R}_{jj'} \cdot \hat{\mathbf{u}}_j \times \hat{\mathbf{u}}_{j'} \qquad \text{(A17)}$$

where $\mathbf{R}_{jj'}$ is the separation vector $(\mathbf{R}_{j'}^0 - \mathbf{R}_j^0)$ between oscillators j and j' and ν_i is the frequency (cm^{-1}) of the ith mode. It is clear from this form of eq A12 that the position of $\mathbf{R}_j^0$ along the bond axis of the oscillator is immaterial and that $\mathbf{R}_j^0$ can be the same point for both atoms in the oscillator, since moving $\mathbf{R}_j^0$ to $\mathbf{R}_j^0 + \lambda\hat{\mathbf{u}}_j$ does not affect the rotational strength. Only pairs of oscillators that are chirally oriented make nonzero contributions in eq A17.

Registry No. 1, 132260-31-2; **2**, 136342-83-1.

General Parameterized SCF Model for Free Energies of Solvation in Aqueous Solution

Christopher J. Cramer*,† and Donald G. Truhlar*,‡

Contribution from the U.S. Army Chemical Research, Development, and Engineering Center, Aberdeen Proving Ground, Maryland 21010-5423, and Department of Chemistry, Supercomputer Institute, and Army High Performance Computing Research Center, University of Minnesota, Minneapolis, Minnesota 55455-0431. *Received March 8, 1991*

Abstract: We present a new general parameterization for aqueous solvation free energies of molecules and ions in aqueous solution. It is obtained by extending a semianalytic treatment of solvation recently proposed for use with molecular mechanics and liquid simulations by Still et al. As extended here, the solvation terms are included in a Fock operator. The model incorporates reaction field polarization effects through the generalized Born functional with charges obtained by AM1 molecular orbital calculations, and it includes cavitation, dispersion, and hydrophobic effects through an empirical function of solvent-accessible surface area. A general parameter set, including parameters for H, C, N, O, F, S, Cl, Br, and I, has been obtained by considering a data set consisting of 141 neutral molecules, 10 cations, and 17 anions. The neutral molecules include alkanes, cycloalkanes, alkenes, arenes, alkynes, ethers, heterocycles, carboxylic acids, esters, nitriles, aldehydes, ketones, alcohols, amines, nitro compounds, sulfides, thiols, halides, and polyfunctional compounds. The general parameterization is called Solvation Model 1, and it is particularly well suited for chemical reaction dynamics and reaction intermediates. We also discuss how the model may be refined for solvation free energies for stable neutral molecules.

1. Introduction

Computational chemistry is continually improving, not only in its ability to correlate experimental trends, but also in the ability to predict qualitative and sometimes quantitative features of structures and reactions not yet observed experimentally. While the advances in ab initio chemistry are dramatic, especially for small molecules,[1] the advances in semiempirical methods, both molecular orbital theory[2] and molecular mechanics,[3] have had an impact on a broader range of chemistry, and these are still the methods of choice for large molecules such as those involved in biochemical processes. Just as the usefulness of ab initio techniques has been closely tied to the availability of well-tested general basis sets[4] and widely applicable computer programs[4] with analytic gradient techniques for stationary point analysis,[5] the revolution in usefulness of semiempirical computational techniques has been closely tied to well-tested general parameterizations,[6-10] such as Austin Model 1 (AM1)[7] and the MM2 force field,[9] and—again—to widely available general computer programs[11-13] with efficient stationary point analyses.[14]

One difficulty that still persists and greatly limits the applicability of computational chemistry techniques is the expense of including solvent effects. Simulations involving large numbers of explicit water molecules[15-18] have proved their usefulness but remain expensive and susceptible to errors in potential energy functions. A complementary approach that should lead to faster progress for some problems is a general parameterization (in the

† U.S. Army Chemical Research, Development, and Engineering Center.
‡ University of Minnesota.

(1) (a) *Comparison of Ab Initio Quantum Chemistry with Experiment for Small Molecules*; Bartlett, R. J., Ed.; D. Reidel: Dordrecht, 1985. (b) *Supercomputer Algorithms for Reactivity, Dynamics, and Kinetics of Small Molecules*; Lagana, A., Ed.; Kluwer: Dordrecht, 1989.
(2) (a) Pople, J. A.; Beveridge, D. L. *Approximate Molecular Orbital Theory*; McGraw-Hill: New York, 1970. (b) Naray-Szabo, G.; Surjan, P. R.; Angyan, J. G. *Applied Quantum Chemistry*, Reidel: Dordrecht, 1987.
(3) Burkert, U.; Allinger, N. L. *Molecular Mechanics*; American Chemical Society: Washington, DC, 1982.
(4) Hehre, W. J.; Radom, L.; Schleyer, P. v. R.; Pople, J. A. *Ab Initio Molecular Orbital Theory*, John Wiley & Sons: New York, 1986.
(5) (a) Pulay, P. *Mol.Phys.* **1969**, *17*, 197. (b) Schlegel, H. B.; Wolfe, S.; Bernardi, F. *J. Chem. Phys.* **1975**, *63*, 3632.
(6) (a) Bingham, R. C.; Dewar, M. J. S.; Lo, D. H. *J. Am. Chem. Soc.* **1975**, *97*, 1294. (b) Dewar, M. J. S.; Thiel, W. *J. Am. Chem. Soc.* **1977**, *99*, 4899.
(7) Dewar, M. J. S.; Zoebisch, E. G.; Healy, E. F.; Stewart, J. J. P. *J. Am. Chem. Soc.* **1985**, *107*, 3902.
(8) Stewart, J. J. P. *J. Comput. Chem.* **1989**, *10*, 209, 221.
(9) Allinger, N. L. *J. Am. Chem. Soc.* **1977**, *99*, 8127.
(10) Allinger, N. L.; Yuh, Y. H.; Li, J.-H. *J. Am. Chem. Soc.* **1989**, *111*, 8551.
(11) Liotard, D. A.; Healy, E. F.; Ruiz, J. M.; Dewar, M. J. S. AMPAC, version 2.1 (Quantum Chemistry Program Exchange program 506). *QCPE Bull.* **1989**, *9*, 123.
(12) (a) Stewart, J. J. P. *J. Comput.-Aided Mol. Des.* **1990**, *4*, 1. (b) Stewart, J. J. P. MOPAC, version 6.0 (Quantum Chemistry Program Exchange program 455). *QCPE Bull.* **1990**, *10*, 86.
(13) Allinger, N. L.; Yuh, Y. H.; Gensmantel, N. P. *MM2* (Quantum Chemistry Program Exchange program 501). *QCPE Bull.* **1985**, *5*, 139.

0002-7863/91/1513-8305$02.50/0